SEMICONDUCTOR GAS SENSORS AS AN EXAMPLE OF THICK-FILM TRANSDUCERS

Vilho Lantto
Microelectronics and Material Physics Laboratories, University of Oulu , Finland

INVITED PAPER
24th International Conference on Microelectronics, MIEL'96
32nd Symposium on Devices and Materials, SD'96
September 25.-September 27., 1996, Nova Gorica, Slovenia

Key words: electronics, microelectronics, thick-film transducers, solid state transducers, thick-film hybrids, semiconductor gas sensors, manufacturing of sensors

Abstract: The research on solid state transducers started in the University of Oulu in the middle of the 1970s, soon after the beginning of the research on thick-film hybrids in the Microeletronics Laboratory. Screen printing is the common technology for the fabrication of both hybrid circuits and thick-film transducers, and has served also as a good possibility for the integration of our thick-film sensors with the necessary signal processing electronics in the form of hybrid modules. A novel double-paste screen-printing method was also developed in our Laboratory for the fabrication of multilayer transducer structures. Pad printing is another thick-film printing technique which offers the possibility for printing fine lines down to a width of about 50 μm. Therefore, it offers a possibility for more dense structures, especially in thick-film sensor arrays. A useful feature of the technique is that it offers a possibility to 3-dimensional printing, which allows a printing for complicated structures.

Semiconductor gas sensors are taken here as an example of our study on thick-film transducers. Our research on semiconductor gas sensors has continued since 1983 and during 1987-1991 we were a research partner in a EUREKA project that aimed to develop semiconductor gas sensors for some practical applications. We have also studied the possibility of using semiconductor gas sensors for monitoring of pollutant gases in combustion emissions and in city air. In a semiconductor gas sensor, the chemical receptor signal on the semiconductor surface is usually transduced through the microstructure of a sintered ceramic into a resistance change of the ceramic. Therefore, different thick-film tehcniques serve as a useful and economic way to produce these devices.

Plinski senzorji - primer razvoja debeloplastnih pretvornikov

Ključne besede: elektronika, mikroelektronika, pretvorniki debeloplastni, pretvorniki polprevodniški, hibridi debeloplastni, senzorji plinov polprevodniški, proizvodnja senzorjev

Povzetek: Z raziskavami na področju pretvornikov smo na Univerzi v Oulu začeli sredi sedemdesetih let, kmalu po začetku raziskav na področju debeloplastnih hibridnih vezij v Laboratoriju za mikroelektroniko. Sitotisk je primerna tehnologija tako za izdelavo hibridnih vezij kakor za izdelavo debeloplastnih pretvornikov in je tako ponujal možnost integracije debeloplastnih senzorjev s potrebno elektroniko za obdelavo signala v obliki hibridnih modulov. Za večplastne strukture pretvornikov smo v našem laboratoriju razvili nov način sitotiska. Za tiskanje ozkih linij s širino do 50 μm pa je primeren gravurni ofset tisk. To omogoča izdelavo še gostejših struktur, kar pride v poštev pri debeloplastnih senzorskih poljih. Uporabna značilnost tega načina tiskanja je, da omogoča tridimenzionalen tisk, kar posebej pride v poštev pri izdelavi zapletenih struktur.

Polprevodniške plinske senzorje smo tukaj vzeli le kot primer preučevanja debeloplastnih pretvornikov. Naše raziskave polprevodniških senzorjev tečejo že od leta 1983 in v letih 1987-1991 smo kot raziskovalni partner sodelovali v EUREKA projektu, katerega cilj je bil razviti polprevodniške plinske senzorje za praktično uporabo. Ravno tako smo preučevali možnost uporabe polprevodniških plinskih senzorjev za nadzor onesnaževanja mestnega zraka. V polprevodniškem plinskem senzorju kemijska sprememba na površini polprevodne keramike povzroči spremembo upornosti. Na ta način lahko različne debeloplastne tehnike uporabimo za učinkovito in ekonomično izdelavo omenjenih elementov.

1. INTRODUCTION

In the literature on sensors, gas sensing devices which consist of a semiconductor between two metal electrodes and which respond to changes in the composition of the surrounding atmosphere with a change in conductance are commonly termed as semiconductor gas sensors. Sometimes they are called as homogeneous gas sensors to distinguish these devices from structured sensors such as gas sensing diodes and field effect transistors. In the case where metal oxides are the gas sensitive semiconductors, the devices are also called oxide, metal-oxide or ceramic gas sensors.

Semiconductor gas sensors utilize the chemical sensitivity of semiconductor surfaces for gas sensing applications. A metal-oxide n-type semiconductor is the usual sensing material in these devices. The sensor detects a gas component due to a change in electrical conductance of a polycrystalline ceramic semiconductor. For the basic understanding of a chemical sensor one needs to separate the receptor function which

recognizes a chemical substance, and the transducer function which transduces the chemical signal into an electric output signal. In a thick-film semiconductor gas sensor, the chemical signal on the semiconductor surface is transduced through the microstructure of the sintered semiconductor into a resistance change. Hence, various grain contacts together with the grain size of the ceramic microstructure are the key concepts for the transducer function /1/. In addition, the mobility of donors, like oxygen vacancies in oxidic semiconductors, may have strong effects on the transducing properties of the sensors /2-4/.

Although the metal oxides used as sensing materials in semiconductor gas sensors have wide band gaps typical of insulators, they possess conductivity in the range of semiconductors due to point defects in the crystal structure. Semiconducting oxides are employed as gas-sensitive resistors for monitoring changes in oxygen partial pressure and small concentrations of impurity gases in air. In the case of response to changes in oxygen partial pressure at temperatures around 700 °C and above, the materials are reflecting the equilibria between the atmosphere and their bulk stoichiometry. The conductance change may then reflect the bulk conductivity effect, i.e. the change in the amount of bulk charge carriers due to native defects related to non-stoichiometry. An n-type binary oxide, TiO_2, is the material which is used commercially for these applications (lambda sensors).

In the case of the second major category which is to monitor the concentration of minor constituents of an atmosphere (normally air), the oxygen partial pressure remains effectively constant. For this type of application, the sensing material is normally held at a relatively lower temperature (below 500 °C), when some surface reactions cause the conductance changes. In sensor applications, the semiconductor material is usually in the form of a thick or thin film over a substrate containing metal film electrodes and a heating resistor. In this structure a high surface area to bulk ratio is achieved.

For the basic understanding of the operation of semicnductor gas sensors, one needs to know both the surface interaction with the active gases (receptor function) and the way to transduce it into conductance signals (transducer function).The dissociation of the oxide lattice (starting at the surface) occurs usually with low oxygen pressure and/or high temperature. In the case of sensing the oxygen partial pressure with the bulk conductivity change (lambda sensor), such a dissociation reaction is the prerequisite for the sensor operation. There is also the possibility that such a reaction will occur on the semiconductor surface at lower temperatures when "surface conductivity" changes are used for sensing. For this case, however, the mechanism most often quoted as the dominant one for detection of reducing or combustible gases in an oxygen containing atmosphere is the adsorption/desorption mechanism in which oxygen is preadsorbed on the surface of the material, trapping electrons from the conduction band, the amount of oxygen chemisorbed being controlled by the oxygen concentration and the amount of reducing gases in the atmosphere.

The surface defect mechanism, provided with the creation and diffusion of oxygen vacancies in the surface layer, is the other suggestion for the receptor function which may also provide a better explanation for some slow response and recovery properties of semiconductor gas sensors. The dissociation problem, which is very important in selection of semiconducting oxides for sensor applications, is closely related to slow and irreversible changes in the conductance of the sensor and limits even some of the most desirable oxides, such as ZnO, in their temperature range of application /5/. Removal of lattice oxygen by a chemical reaction on the oxide surface (CO or hydrocarbons, for example) is another source for the surface defect mechanism. Tin dioxide, SnO_2, has resistant surfaces against irreversible decomposition up to 500 °C and, therefore, it is the usual material in commercial sensors.

2. THICK FILM PRINTING TECHNIQUES

2.1 Screen printing and sensor integration

Thick-film technology based on screen printing serves as an economic way to produce sintered SnO_2 sensors with a high surface area to bulk ratio. The simple structure of a thick-film sensor is shown in Fig. 1(a). A planar ceramic alumina acts as the substrate for the thick-film sensor. Laser machining is used for scoring and drilling the alumina. Both the metal electrode (normally Au) and the SnO_2 layer over the electrode, are made by screen printing on the substrate which has a thick-film Pt heating resistor (around 10 Ω) printed on the reverse side of the substrate.

The gas-sensitive layer is prepared by making the semiconductor powder in the form of a paste suitable for screen printing. Commercial SnO_2 powders of high purity and decomposable salts of tin, such as $SnCl_4.5H_2O$ and $SnSO_2$, have been used in paste making for SnO_2 sensors. In the case when the chloride was used, different conductivity levels were obtained by adding Al or Sb in chloride form to the solution from which tin hydroxide was precipitated and the oxide formed in a calcination step. A surface binder, such as silica, is usually added to the mixture which is formed into the paste. The binder may have a strong effect on the characteristics of the sensor.

There are many procedures to introduce catalysts into the SnO_2 powders used to make thick-film layers. One way is to modify the SnO_2 powder with the catalyst, screen print the layer, and then sinter. Agglomeration of the metal particles into small isles results from this technique.

Screen printing is the common technology for the fabrication of hybrid circuits in addition to thick-film transducers, which has served as a good possibility for the integration of thick-film sensors with the necessary signal processing electronics in the form of a hybrid module. An integration of SnO_2 gas sensor into a screen-printed hybrid module is shown in Fig.1(b). Because of the heating of the sensor up to elevated tem-

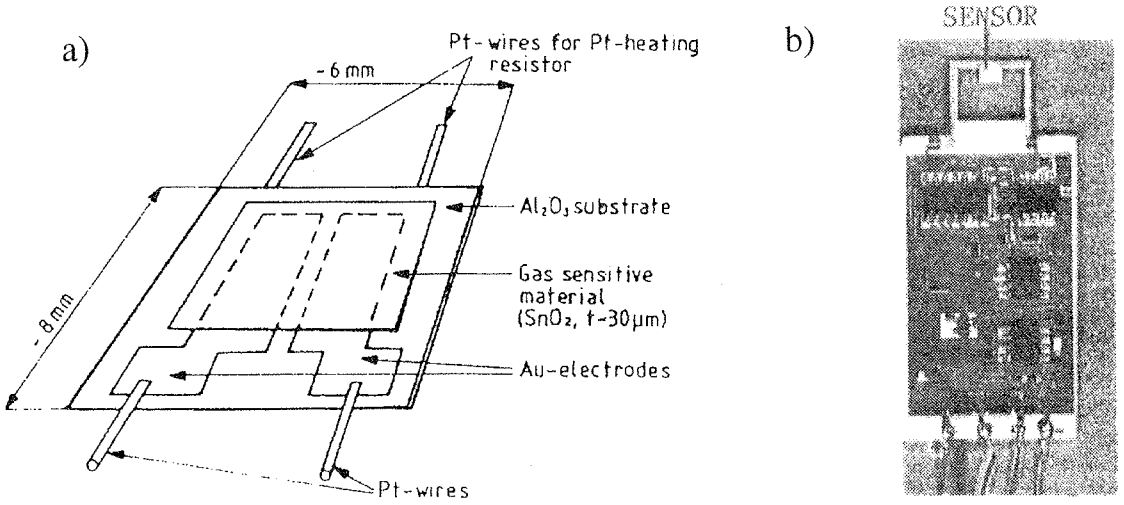

Figure 1: (a) Cross section of an SnO_2 thick-film sensor together with a Pt-heating resistor on the reverse side of an alumina substrate (6x8 mm²). (b) An integration of a thick-film SnO_2 gas sensor (3x3 mm²) with a signal-processing hybrid circuit into a screen-printed hybrid module.

peratures, it is connected to the hybrid circuit only with narrow (about 1 mm) alumina-substrate bridges containing electrodes both for sensing and for the Pt heating resitor on the reverse side. Conductance response is changed to a voltage output by the module.

2.2 Pad printing of one-electrode gas sensors

Standard thick-film technology based on screen printing is practicable for many sensor applications, but has also some limitations compared with thin-film techniques. The narrowest line widths obtained by standard screen printing are about 100 μm and this has some limitations for sensor applications. Pad printing or gravure-offset printing is a novel thick-film printing technique which offers the possibility of printing conductor lines down to a width of 50 μm /6/. The principle of gravure-offset printing is described in Fig. 2. The desired pattern which is etched in a gravure plate is first flooded

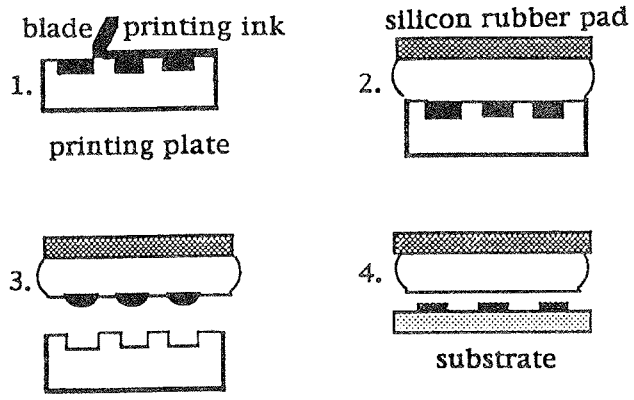

Fig. 2: Description of the principle of pad printing or gravure-offset printing.

with ink and then scraped clean so that ink remains only in the engraved pattern. Subsequently, the pattern is picked up and transferred from the plate by a flexible silicone rubber pad when it is pressed against the substrate. In order to get a good print, it is necessary to optimise all the parameters of the printing process. Typically the depth of the engraved pattern in the plate after etching is 15-25 μm. The smoothness of the substrate surface has a considerable effect on the quality of printing trace, but generally all thick-film substrates can be used. A useful feature of gravure-offset printing is that the technique offers a possibility of 3-D printing, which allows the printing of very complicated structures.

One-electrode semiconductor gas sensors are taken here as an example of the use of pad printing in sensor fabrication. In a typical sensor construction, the sensing semiconductor is between two metal (Au or Pt) electrodes and a third metal electrode, usually platinum, is used for the heating of the sensor device (Fig.1). In the one-eletrode construction /6/, a thin platinum-wire (ϕ = 20 μm) spiral is embedded inside a sintered oxide-semiconductor buttom. Figure 3(a) shows a construction of the one-electrode sensor /6/. The one-electrode spiral acts both as the heating resistor and measuring electrode, and the sensor works under a stabilized constant current feed. The function of the one-electrode sensor is based on shunting of the heating resistor as a result of a gas interaction with the oxide semiconductor. The equivalent circuit in Fig. 3(b) describes the operation of the sensor. At the gas exposure, the sensor response is obtained as a voltage change ΔV_M. In the case of a reducing gas like CO with an n-type semiconductor, a decrease of the overall resistance R (parallel resistance of the Pt resistor R_H and oxide-semiconductor shunt resistor R_S), decreases the heating power RI^2 (with a constant current I) and the operation temperature of the sensor.

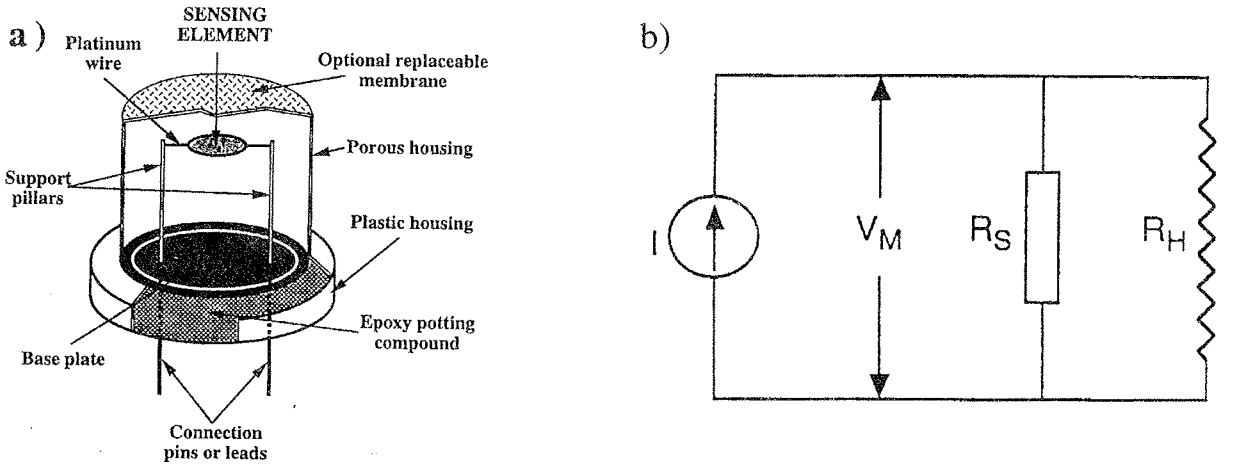

Fig. 3: (a) Structure of a bulk-type one-electrode semiconductor gas sensor where a thin Pt-wire spiral is embedded inside a sintered oxide-semiconductor buttom. (b) Equivalent circuit for the operation of the one-electrode semiconductor gas sensor. R_H and R_S are the Pt-heating resistor and shunting-semiconductor resistor, respectively.

Both screen printing and pad printing were used in the fabrication of our one-electrode thick-film sensors to print Pt thick-film resistors over alumina substrates. The structure of these two sensor types with screen-printed (I-type) and pad-printed (II-type) Pt resistors are shown in Figs. 4(a) and 4(b), respectively. Screen printing is used for the printing of the sensing SnO_2 thick film over the Pt resistor in both sensor types.

The practical limit for the minimum line width in screen printing is currently about 100 μm. This makes possible to print Pt resistors with resistance only up to few tens of ohms over a small substrate area (about 5x5 mm^2 or less) of the sensor. The shunting semiconductor thick-film resistor should have a resistance value of the same order with that of the Pt resistor at the operation temperature. That means, in the case of screen-printed Pt resistors, a heavy doping of the sensing oxide, e.g., SnO_2 with a group V element such as Sb. However, the heavy doping may change the sensing properties of the oxide film and impair the performance of the sensor. Therefore, an increase of the resistance of the Pt thick-film resistor is of great practical importance for the fabrication of our sensor prototype.

Pad printing offers possibilities for fine-line printing which makes possible to increase substantially the resistance of the Pt resistors. Sinterable Pt pastes for the resistor printing were modified by adding an appropriate mixture of organic binder and solvents to make the viscosity suitable for pad printing. Typically, the thickness of the fired conductors printed by gravure-offset technique ranges from 1 to 3 μm depending on the properties of the paste and the depth of engraving on the printing plate. The line width of the Pt resistor in Fig. 4(b) was possible to press down to about 50 μm. Then, pad printing made possible to produce Pt thick-film resistors with resistance up to kΩ and avoid the heavy doping of the sensing SnO_2 films with donors.

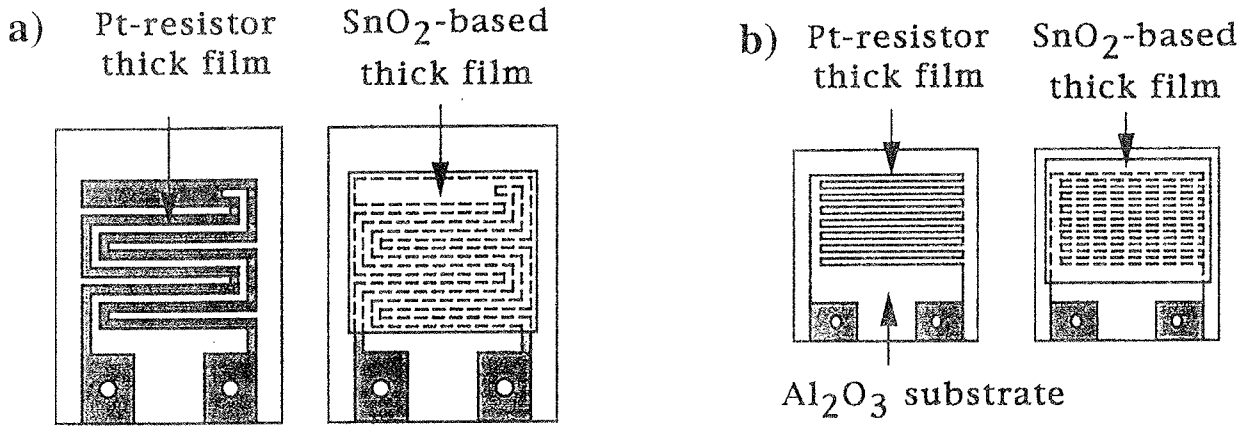

Fig. 4: Structure of thick-film one-electrode semiconductor gas sensors with a) screen-printed (I-type) and b) pad-printed (II-type) Pt thick-film resistors on alumina substrate. The SnO_2 sensing layer over the Pt resistor is screen printed in both sensor types. The substrate areas were 6x8 mm^2 and 5x5 mm^2 with the line width of Pt resistors of about 100 and 60 μm, respectively, for I-type and II-type sensors /6/.

The response of two one-electrode thick-film sensors with the same Ag-doped SnO_2 sensing layer to different amounts of H_2S (1,2,3, and 4 ppm) in dry synthetic air is shown as a function of time in Figs. 5(a) and 5(b), respectively, for sensors with screeen-printed (I-type) and pad-printed (II-type) Pt-heating resistors. Heating powers were adjusted in pure synthetic air to correspond the operation temperature of 450°C for both sensors. The sensor with the pad-printed Pt resistor (II-type) is sensitive to H_2S from 1 ppm level up, but the sensor with screen-printed Pt resistor (I-type) is not at all suitable for H_2S sensing in the low ppm range. The low resistance of the screen-printed Pt resistor as compared with that of the shunting SnO_2 layer is the reason for that behaviour. In the case of the II-type sensor in Fig. 5(b), the Pt-resistor resistance is comparable with the shunting resistance.

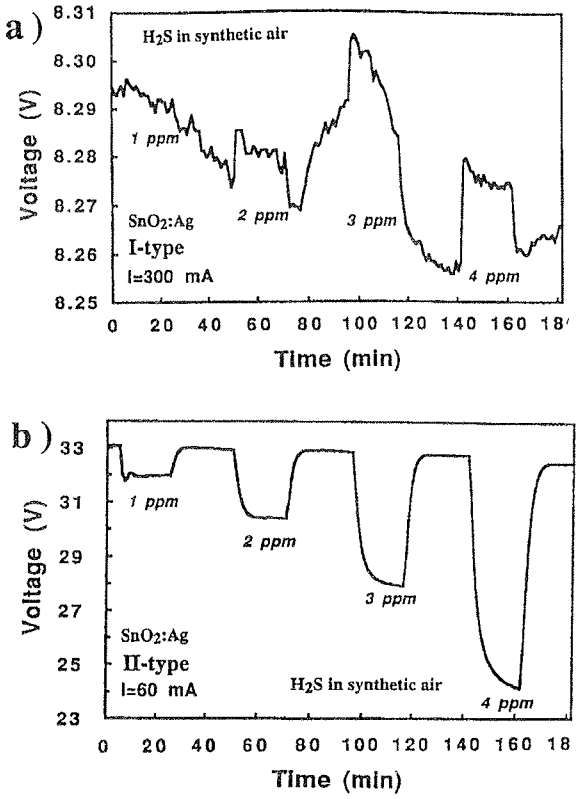

Fig. 5: Voltage response of (a) a I-type and (b) II-type sensor with Ag-doped SnO_2 sensing layer to 1, 2, 3 and 4 ppm of H_2S in dry synthetic air.

3. CONDUCTANCE OF SINTERED SnO_2 THICK FILMS

It is well known that negative charges accumulate on the surface of n-type semiconductor materials like SnO_2 in oxygen-containing atmospheres. According to the general electronic theory of chemisorption this is due to discrete energy levels introduced by oxygen within the band gap. This negative charge generates a depletion layer and a Schottky potential energy barrier on the semiconductor surface which has a very pronounced effect on the electrical conductivity if the material is in the form of porous ceramics, as in the case of SnO_2 thick films. The vibrating capacitor (Kelvin probe) seems to be a useful tool for measuring work-function changes also over the surface of thick-film samples /7/. Result of simultaneous response of work function and resistivity of some SnO_2 based thick-film samples to H_2 at three different temperatures of 420, 500 and 620 K /7/ support the Schottky barrier model for the conductance response. The depletion mode seems to prevail on SnO_2 surfaces in the presence of small H_2 concentrations in air, although in the UHV (ultra high vacuum) case, ionized surface donors, e.g., adsorbed hydrogen atoms or oxygen vacancies may turn the surface to the accumulation mode /8/. In the case of surface depletion, the work function eV_K of an n-type semiconductor increases by the amount of the Schottky barrier eV_S, as is sketched in Fig. 6(a). A decrease of the negative surface charge

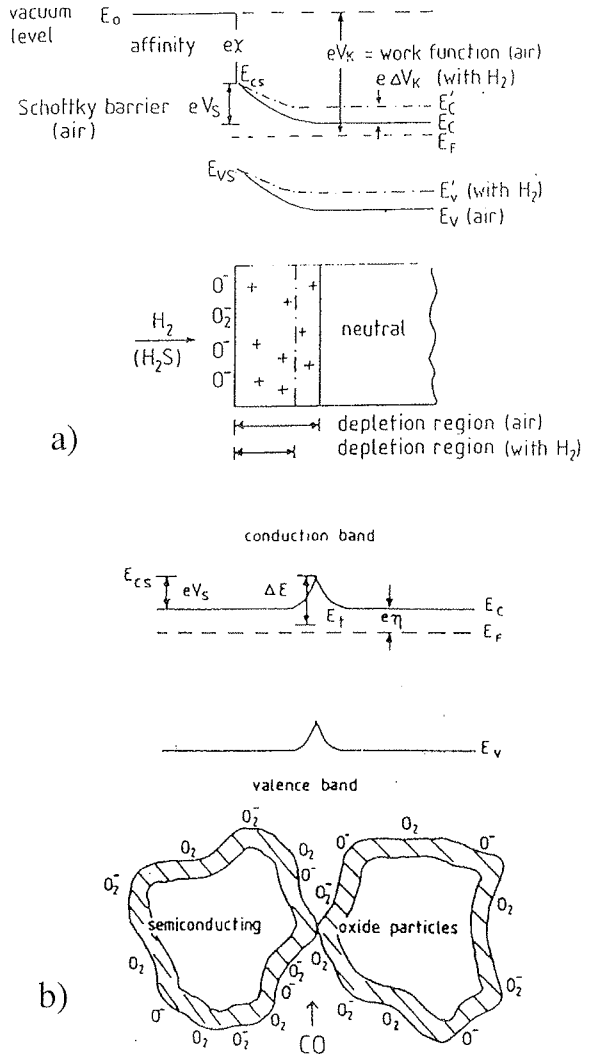

Fig. 6: (a) Illustration of the effect of negative surface charge (oxygen ions) and the Schottky barrier eV_S on the work function eV_K on the surface of an n-type semiconductor. (b) Schematic picture of the contact between two semiconducting oxide particles where the negative surface charge due to ionosorbed oxygen species generates a depletion layer and a Schottky barrier, as is sketched in the upper band diagram.

(adsorption/desorption mechanism) as a consequence of catalytic reactions, e.g., H_2 in the figure, also decreases the work function (by $e\Delta V_K$ in Fig. 6(a)). A change of the work function may origin also from the surface defect mechanism, since a release of lattice oxygen by a reducing agent such as CO at the surface may create a dipole layer at the ionic surface.

A schematic picture of the contact between two semiconducting oxide particles in sintered thick films is shown in Fig. 6(b) where the negative surface charge due to ionosorbed oxygen species generates a depletion layer and a Schottky potential energy barrier eV_S as is sketched in the upper band diagram in the figure. An energy level E_t introduced by oxygen within the band gap, near the Fermi level E_F in the surface region, is also shown in Fig. 6(b), although there are, of course, different levels related to different oxygen species (O_2^-, O^-). Reducing agents such as H_2 (or CO) in the ambient remove the negative charge from the surface by catalytic oxidation reactions (adsorption/desorption model) which have the effect to decrease the Schottky barrier eV_S and increase the conductance of the sample.

The Schottky barriers at intergranular contacts in sintered samples (Fig. 6(b)) dominate the resistance, since the electrons must overcome a substantial energy barrier eV_S in order to cross from one grain to another. In a compressed powder pellet, at least, the same constant surface barrier eV_S (Fig. 6(a)) may be assumed to exist on both sides of the intergranular contact in Fig. 6(b) and, as a first approximation, the conductance G at a temperature T may be described by the equation

$$G = G_0 \exp(-eV_S/kT) \qquad (1)$$

where G_0 may be considered as a factor which includes the bulk intragranular conductivity and geometrical effects. In order that the form of eqn. (1) is valid, the voltage drop at each intergranular contact must be less than kT/e so that the voltage dependence of the current is ohmic.

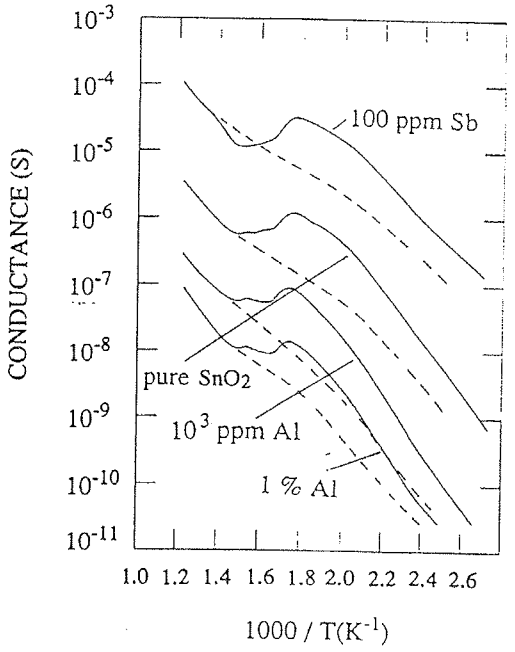

Fig. 7: Conductance of pure, Sb- and Al-doped SnO_2 thick-film samples with Au electrodes in dry synthetic air as a function of inverse temperature, measured at a cooling (- - -) and heating (——) rate of 2.4 Kmin^{-1} /9/.

Figure 7 shows measured conductance values of pure, Sd-doped and Al-doped SnO_2 thick-film samples in dry synthetic air (humidity few ppm) between 100 and 550°C during heating and cooling with a rate of 2.4 Kmin^{-1}/9/. The Arrhenius plots with the irreversible conductance behaviour in Fig. 7 are very characteristic for sintered SnO_2 samples in dry ambient atmosphere. During heating, the conductance of all the four samples with very different surface concentration of electrons turn to decrease at exactly the same temperature of 280°C.

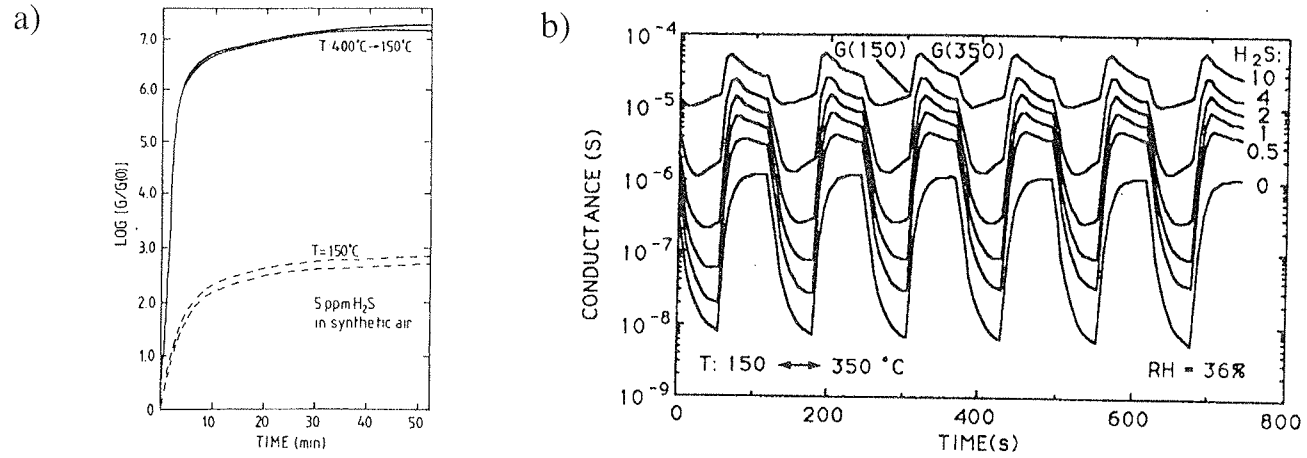

Fig. 8: (a) Conductance with time of two SnO_2 thick-film sensors in synthetic air after introduction of 5 ppm of H_2S at time zero on equilibrium surfaces at 150°C (- - -) and on non-equilibrium surfaces rapidly cooled from 400 to 150°C (——)/10/. (b) Conductance response of an SnO_2 thick-film sensor in the temperature-pulsed mode between 150 and 350°C to 0, 0.5, 1, 2, 4 and 10 ppm of H_2S in air with r.h. of 36 %.

Therefore, the behaviour origins from structural surface changes which naturally relate to the lattice-oxygen balance at ionic oxide surfaces. A clear understanding of the unusual sigmoid variation of conductance with inverse temperature were very desirable, since some "sensitization" of sensors seems to relate to this phenomenon. After a rapid cooling from temperatures above the downward deflection temperature (280°C), sensors are usually much more sensitive at low temperatures. Fig. 8(a) shows conductance response of two SnO_2 thick-film sensors in dry air after introduction of 5 ppm of H_2S at time zero on equilibrium surfaces at 150°C and on non-equilibrium surfaces rapidly cooled from 400 to 150°C /10/. In the case of equilibrium surfaces, the sensors were allowed to remain at 150°C for two days before the measurements, while in the case of non-equilibrium surfaces, temperature of the sensors was raised to 400°C and they were allowed to remain at this temperature for about 20 h. This makes possible a temperature-pulsed mode of sensor operation (Fig. 8(b)) /11/.

4. COMPUTATIONAL APPROACH FOR CHEMICAL SURFACE ACTIVITY

A model approach for the chemical response of a semiconductor surface is based (1) on a possible ionic response of the semiconductor bulk on changing internal electric fields, (2) on rate equations to describe electron transfer processes between the semiconductor- bulk Bloch states and surface adsorbates, and (3) on localized electron interactions at the surface. High-speed computers of today make possible to attack to all these three prerequisities for a proper dynamical treatment of the chemical surface activity /12/. At elevated temperatures, the grains in a ceramic semiconductor may behave as a solid electrolyte where dopant distributions inside the grains change with changing electrical potentials. Now, the electrical potential inside a grain is a solution of the Poisson-Boltzmann equation for which a computational approach is necessary, e.g., in the spherical grain geometry. It was found /13/ very large differences in the potential distribution inside a grain between the two cases with frozen and mobile donors, respectively. Expressions which are similar to those for the generation-recombination processes in semiconductors (Shockley-Hall-Read theory) can be used to describe the variation of electron transfer rates versus surface potential for MOS diodes. In our simulation procedure for electron transfer rates between the bulk Bloch states and surface adsorbates, we have adopted similar expressions to describe electron capture rates from the bulk conduction band, e.g., to oxygen surface species /14/.

A computational approach for localized electron interactions at the semiconductor surface is described here. A surface structure and adsorbates on the surface can be modeled either with a cluster, a chunk of surface, or a slab model, an infinite periodic system with a unit cell describing the surface structure of interest. Cluster models, which are often most convenient to describe localized structures and phenomena ignore the periodicity, and thus, yield a molecular electronic structure with discrete one-electron levels. If the band structure of the continuum levels at the surface is essential, one has to invoke the slab models and intrinsically periodic methods.

The case chosen to present here is stannic oxide SnO_2 and its (110) surface to illustrate some basic aspects of the gas-sensor surface phenomena. SnO_2 is one of the most applied material and the stable (110) face is its nonpolar surface that can be studied even in its bulk derived geometry without relaxation. Nitrogen oxide (NO molecule) is taken as an example of the adsorbate and chromium (Cr atoms) as an example of an impurity used to dope the SnO_2 semiconductor. The adsorption and doping effects can be examined as local phenomena to the extent where a cluster model in Fig. 9 is adequate /15/.

For such a large cluster the density functional method with the local density approximation (LDA) is the method of choice, if an ab initio level approach is desired. There are a collection of good commercial software, of which we have mostly been using DMol and DSolid from Biosym, but also academic codes have

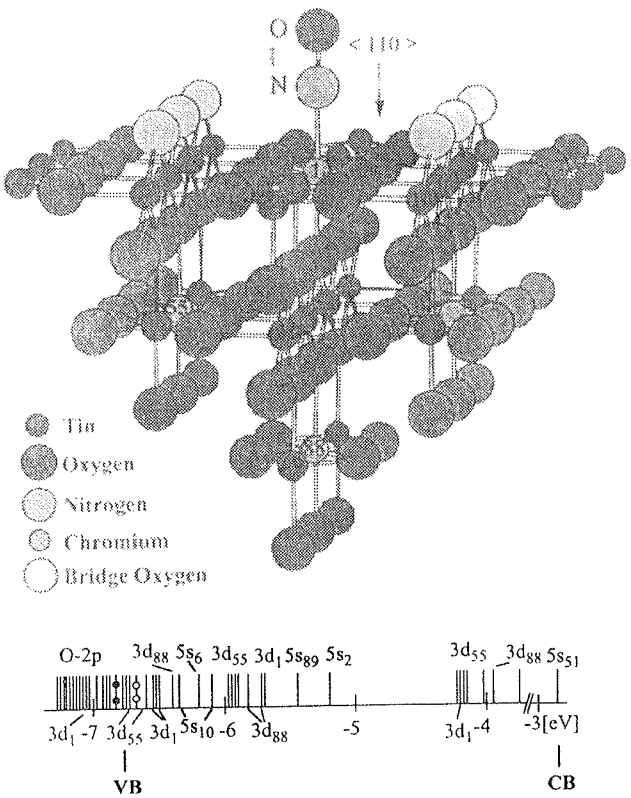

Fig. 9: Geometry of an $Sn_{28}O_{71}Cr_4$ cluster (in C_{2v} symmetry) modeling the (110)-1x1 surface of SnO_2. Cr atoms as dopants substitute some of the Sn at 1,55 (and its C_{2v} symmetry site) and 88 sites, and a NO molecule is placed as an adsorbate on a probable surface site. The bridge oxygen sites on the surface are assumed to be occupied in usual conditions. The calculated "molecular" one-electron level structure (without the adsorbate) at the "band-gap" region is shown below. Part of the population analysis (the strongest atomic orbital component of each level) is also shown /15/.

been employed for more specific purposes. Very briefly, these SCF ab initio methods are based on the linear-combination-of-atomic-orbitals (LCAO) theory and basis functions in numerical form from atomic and ionic calculations.

The band gap of bulk SnO_2 is about 3.6 eV, and roughly, the valence band maximum is created from 2p levels of oxygen and the conduction band minimum from 5s levels of tin. There are some surface states (levels) in the band gap, of which many are related to the missing bridge oxygen atoms. There are also gap levels arising from the finite size effect of our small cluster, i.e., there is more surface than only the intended (110) surface. All this can be nicely seen in the level map in Fig. 9. Chromium impurities in SnO_2 have a strong effect on the electrical properties both in the bulk and at the surface. It is a consequence of Cr 3d levels, which emerge in the band gap. The bulk impurities cause the deep levels near the valence band and the surface impurities create levels in the middle part of the gap. Both of these level types behave as conduction electron traps in an n-type SnO_2 semiconductor. This explains, for example, why Cr impurities have so strong effect on the conductivity of polycrystalline SnO_2 film.

Chromium impurities in SnO_2 have a strong effect on the catalytic properties, too. It seems that the high reactivity of Cr ions at the surface is responsible for the enhanced adsorption and dissociation of NO. We can start the analysis from the one-electron orbitals of the NO molecule, shown in Fig. 10.

The bond in the NO is formed by the fully occupied bonding 1π and 5σ orbitals and weakened by one electron in the antibonding $2\pi^*$ level. Thus, the bond is something between the triple bond of N_2 and double bond of O_2. Further occupation of antibonding levels would weaken the bond, and in fact, dissociation of free NO implies degeneration of the 1π, 5σ, $2\pi^*$ and $6\sigma^*$

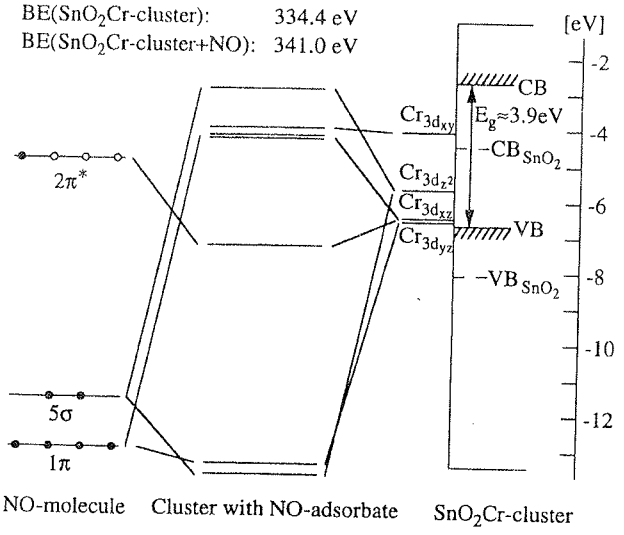

Fig. 10: Calculated one-electron levels of free NO molecule and the SnO_2-Cr cluster with and without the NO adsorbate. Only the levels originating from NO or Cr are shown explicitly /15/.

levels to the atomic 2p levels, thus decreasing (increasing) the occupation of bonding (antibonding) levels. This is also the mechanism of the NO dissociation on the Cr activated SnO_2 surface, though energetically much more favorable than the dissociation of free NO. In Fig. 10 it is seen how NO 1π, 5σ, $2\pi^*$ orbitals hybridize with the Cr 3d levels leading to slightly decreased occupation of bonding and strongly increased occupation of antibonding molecular orbitals. This is actually the conventional picture of transient formation of an NO^- ion with increased occupation of $2\pi^*$ in catalytic reduction of NO.

Surface relaxation and even reconstructions are known to be large for some compound semiconductor surfaces. Usually they are also essential in tuning the catalytic activity through adjusting the polarity and dangling bonds and oher factors in the surface density of states. In the present case removal or adding the bridging oxygen atoms in Fig. 9, change the surface relaxation considerably. For instance, we want to establish the role of the bridging oxygen atoms in the irreversible conductance behaviour of different doped SnO_2 samples in Fig. 7. In the case of CO exposure, for instance, conductance changes of the samples in Fig. 7 follow the exposure only at temperatures above 280 °C, and now the structural surface changes have also a close relation to the catalytic properties of the surfaces.

Though static geometries give certain understanding of surface processes in the long run with increasing computational resources it will be possible to study more dynamical aspects at the ab initio level. This could be done by ab initio molecular dynamics or through evaluation of potential energy hypersurfaces, for example /16/.

5. AN EXAMPLE OF H_2S MONITORING AS AN AIR POLLUTANT

An important application of gas sensors is for the measurement of air pollutants, concentrations of which are usually in the low ppb range. To obtain good sensitivity and selectivity to a certain polluting gas with semiconductor gas sensors is not very straightforward at the moment. We have used some Ag-doped SnO_2 sensors to monitor the H_2S concentration as a polluting agent in the atmosphere of the city Oulu /11, 17, 18/. A sensor array construction consisting of few SnO_2 sensors has been installed at the city air-pollution monitoring station where H_2S and SO_2 cencentrations are being simultaneously recorded by commercial analysing equipment based on coulometric titration together with the conductance signals from the semiconductor gas-sensor array.

The southern part of the city Oulu was an ideal place for such a test. The schematic location of the city monitoring station (centre of the circle) is shown in Fig. 11 together with the city map and the distribution of wind directions in the city area. The most probable sources for polluting gases have also been marked on the city map. There are three concentrated sources of air pollution between the West North West (WNW) and the North North East (NNE) while the other directions are clean. The wind has about 40 % probability of blowing from the directions between WNW and NNE.

The recorder trace of a mV recorder was used to describe the conductance response of the SnO_2 sensors together with the H_2S and SO_2 outputs from the commercial analysers. The SnO_2 sensors, differently doped with Ag and mixed with Al_2O_3, were running at a constant temperature of 250°C during the monitoring. A recorder trace covering a day interval from the city station is shown in Figs. 2(a) and (b). The time period in Fig. 12(a) covers 24 h starting at 4.00 am (16 th December, 1990). During that time the wind turned from W to SSE, passing through the directions of the three main air-polluting sources in the city (a cellulose factory in WNW, the city heat power plant in NNW and a chemical factory in NNE). Half-hour average values of H_2S pollution in $\mu g/m^3$, available in a printed form from the station, are also shown around each hour in Fig.12(a). The relation 1 ppb ≈ 1.35 $\mu g/m^3$ holds for H_2S in atmospheric air around 20°C. The highest H_2S pollution peak (106 $\mu g/m^3$) appeared around 5.00 am from the cellulose factory. Between 2.00 pm and 11.00 pm, the origin of the H_2S pollution was the chemical factory and the half-hour average values of the H_2S pollution increased up to 8 $\mu g/m^3$. As is shown in Fig. 12(a), all the three SnO_2-based sensors are very sensitive to H_2S pollution. They also show conductance peaks between 8.00 am and 12.00 am when the wind blew from the direction (NNW) of the city heat power plant and the commercial analyser showed zero H_2S pollution. The same situation appears also in Fig. 12(b), where the wind stayed in clear directions all day and the readings from the commercial H_2S analyser were zero. In spite of that, the semiconductor sensors show some conductance peaks, especially around midday. It seems that the sensors are sensitive to H_2S pollution even in the sub-ppb range.

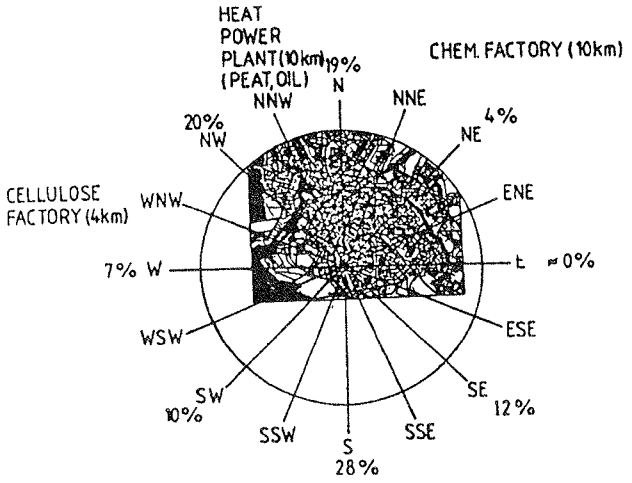

Fig. 11: Location of a pollution monitoring station (centre of the circle) shown on the city map of Oulu, Finland. The distribution of wind directions and three main polluting sources are also shown /17/.

6. SUMMARY

Semiconductor gas sensors are discussed as an example of research with different thick-film transducers in the Microelectronics and Material Physics Laboratories of the University of Oulu, Finland. The use of different thick-film printing techniques in the fabrication of semiconductor gas sensors is also described. An example is given of the use of the common screen-printing technology for the integration of a semiconductor thick-

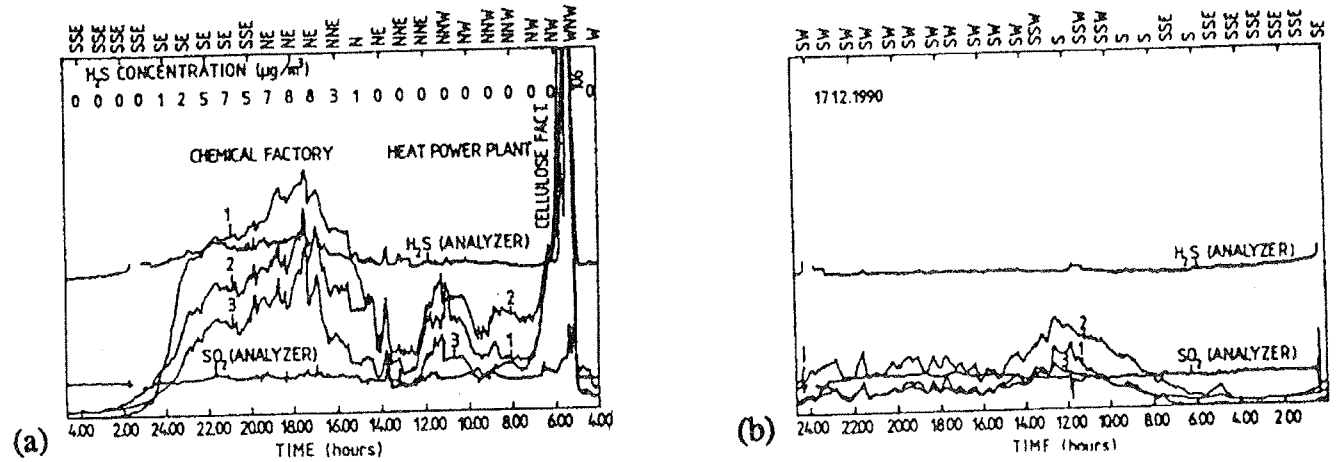

Fig. 12: (a) Recorder trace of 16th December, 1990 (starting 4.00 am) from the city air-monitoring station. Curves numbered 1 to 3 show the conductance response of the three differently doped SnO_2 + (Ag + Al_2O_3) sensors together with the outputs of the commercial H_2S and SO_2 analyser. The time scale increases from right to left and the wind directions, together with the half-hour average concentrations of H_2S, are shown at the top /11/. (b) Recorder trace of 17th December, 1990 from the city station with the same symbols as in (a). The wind was in clean directions between SE and SW all the time /11/.

film gas sensor with a hybrid circuit for signal processing. Semiconductor gas sensors in the form of the one-electrode construction are used to describe the possibilities of pad printing in the fabrication of thick-film transducers. Conductance response of semiconductor thick-film gas sensors to different ambient atmospheres is also discussed and a computational approach for the chemical activity of semiconductor surfaces is described. H_2S monitoring as an air pollutant in city air is taken as an example of the application of semiconductor gas sensors.

7. ACKNOWLEDGEMENTS

I express my warm gratitlude to Mr. Tuomo Rantala and Dr. Tapio Rantala and to my other coworkers for the possibility to use our common research results in this presentation.

8. REFERENCES

/1/ N. Yamazoe, "New approaches for improving semiconductor gas sensors", Sensors and Actuators B, 5, 1991, 7-19.

/2/ D. Kohl, in Gas Sensors, edited by G. Sberveglieri, Kluwer, Dordrecht, 1992, pp. 43-88, ISBN 0-7923-2004-2.

/3/ V. Lantto and T.S. Rantala, "Computer simulation of the surface energy barrier of oxidic semiconductors with mobile donors", Sensors and Actuators B, 18-19, 1994, 711-715.

/4/ T.S. Rantala and V. Lantto, "Some effects of mobile donors on electron trapping at semiconductor surfaces", Surface Science, 352-354, 1996, 765-770.

/5/ M.J. Madou and S.R. Morrison, Chemical Sensing with Solid State Devices, Academic Press, San Diego, 1989, ISBN 0-12-464965-3.

/6/ V. Golovanov, J.L. Solis, V. Lantto and S. Leppävuori, "Different thick-film methods in printing of one-electrode semiconductor gas sensors, Sensors and Actuators B, in press.

/7/ J. Mizsei and V. Lantto, "Simultaneous response of work function and resistivity of some SnO_2-based samples to H_2 and H_2S", Sensors and Actuators B, 4, 1991, 163-168.

/8/ G. Heiland and D. Kohl, in Chemical Sensor Technology, Vol. I, edited by T. Seiyama, Kodansha, Tokyo and Elsevier, Amsterdam, 1988, pp. 15-38, ISBN 0-444-98901-3.

/9/ V. Lantto and V. Golovanov, "A comparison of conductance behaviour between SnO_2 and CdS gas-sensitive films", Sensors and Actuators B, 24-25, 1995, 614-618.

/10/ V. Lantto, P. Romppainen, T.S. Rantala and S. Leppävuori, "Equilibrium and non-equilibrium conductance response of sintered SnO_2 samples to H_2S", Sensors and Actuators B, 4, 1991, 451-455.

/11/ A. Harkoma-Mattila, T.S. Rantala, V. Lantto and S. Leppävuori, "Sensitivity and selectivity of doped SnO_2 thick-film sensors to H_2S in the constant- and pulsed-temperature modes", Sensors and Actuators B, 6, 1992, 248-252.

/12/ T.S. Rantala and V. Lantto, "Computational approach for the chemical sensitivity of oxide and sulphide semiconductor surfaces", Physica Scripta, in press.

/13/ T.S. Rantala and V. Lantto, "Effects of mobile donors on potential distribution in grain contacts of sintered ceramic semiconductors", J. Appl. Phys., 79, 1996, 9206-9212.

/14/ T.S. Rantala, V. Lantto and T.T. Rantala, "Rate equation simulation of the height of Schottky barriers at the surface of oxidic semiconductors", Sensors and Actuators B, 13-14, 1993, 234-237.

/15/ T.S. Rantala, V. Lantto and T.T. Rantala, "A cluster approach for modelling of surface characteristics of stannic oxide", Physica Scripta, T54, 1994, 252-255.

/16/ T.S. Rantala, V. Lantto and T.T. Rantala, "Semiconductor gas sensor - an electronic nose", CSC News, 8, No 2, 1996, 23-26.

/17/ V. Lantto and J. Mizsei, "H_2S monitoring as an air pollutant with silver-doped SnO_2 thin-film sensors, Sensors and Actuators B, 5, 1991, 103-107.

/18/ J. Mizsei and V. Lantto, "Air pollution monitoring with a semiconductor gas sensor array system, Sensors and Actuators B, 6, 1992, 223-227.

Dr. Vilho Lantto
University of Oulu
Microelectronics and Material Physics Laboratories
Linnanmaa, FIN-90570 Oulu, Finland;
tel.: +358 8 553 2710
fax: +358 8 553 2728
e-mail: vila@ee.oulu.fi

Prispelo (Arrived): 03.11.1996 *Sprejeto (Accepted): 19.11.1996*